Design of a Robust Decoupling Matrix for High Field Parallel Transmit Arrays

Zohaib Mahmood[1], Bastien Guérin[2], Boris Keil[2], Elfar Adalsteinsson[1,3], Lawrence L. Wald[2,3], and Luca Daniel[1]

[1]*Dept of Electrical Engineering & Computer Science, Massachusetts Institute of Technology, Cambridge, MA, United States,* [2]*A. A. Martinos Center for Biomedical Imaging, Dept. of Radiology, Massachusetts General Hospital, Charlestown, MA, United States,* [3]*Harvard-MIT Division of Health Sciences Technology, Cambridge, MA, United States*

Target audience: RF engineers and MR physicists. **Purpose:** In a coupled parallel transmit array, the power delivered to a channel is partially distributed to other channels because of coupling. This power is dissipated in the circulators and lost for excitation [1]. Most of the existing decoupling methods focus on nearest-neighboring channels [2]. Capacitive ladder networks, [3], which aim at decoupling also distant neighbors are highly sensitive to specific tuning and matching conditions and are rarely used because of this lack of robustness. Simulations in [4,5] show that a decoupling matrix can be inserted between the power amplifiers and the transmit array to achieve ideal decoupling. In addition to mixing the input signals to provide uncoupled B1+ patterns, such matrix also minimizes the power lost in the circulators. In this abstract, we explore several design aspects of the decoupling matrix, including the network topology, robustness and sensitivity to component values by designing a decoupling matrix for a 4-channel coupled array. The 4-channel instantiation is for demonstration and evaluation purposes to illustrate the principles of robustness and topology exploration. The methods presented in this abstract readily scale to any arbitrary number of channels. **Method:** We built a 4-channel parallel transmit head array tuned and matched at 297.2 MHz (7T) with significant coupling between the channels (Fig. 1b). We computed a decoupling matrix, parameterized by its admittance $Y_C = \{Y_{C11}, Y_{C12}, Y_{C21}, Y_{C22}\}$, by minimization of the following least-squares objective:$\|Y_{out} - Y_u\|_2^2$. In this function, Y_{out} is the output admittance of the array in the presence of a decoupling matrix and is given by $Y_{out} = Y_{C11} - Y_{C12}(Y_{C22} + Y)^{-1}Y_{C21}$ and Y_u is the target output admittance matrix, $Y_u = diag\left(\frac{1}{50\,\Omega}\right)$, that reflects perfect decoupling of the coil elements. Y is the admittance matrix of the coupled array. We enforce the decoupling matrix to take the structure shown in Fig 1(c). We found that this structure retained enough degrees-of-freedom needed to achieve good decoupling while reducing the number of reactive elements from $N(2N+1)$ required to implement an arbitrary decoupling matrix, to $N(N+1)$ (N is the number of channels). We also enforced a robustness criterion during the design by optimizing the decoupling matrix in a range of frequencies around the L'armor frequency (6 MHz robustness bandwidth, Fig. 2). Finally, we performed a sensitivity analysis of the final circuit with respect to small variations of the lumped element values (Fig. 2d) by studying the output S-parameters of the array with the decoupling matrix, when the capacitors and inductors values where swept in a -5% to +5% range.

Results and Discussion: We designed two decoupling matrices with and without a robustness criterion. The non-robust decoupling matrix achieved ideal decoupling, Fig 2(a), but had an extremely sharp frequency response. Imposing robustness constraints in the design of the decoupling matrix yielded a broader response, Fig 2(b), making the circuit more tolerant to component value variations. Additionally, Fig 2(c) shows that this robust design can be implemented in practice using standard C and L values (see also Fig 1(d)). Our sensitivity analysis confirmed that the quality of the decoupling was indeed robust to variation of most of the lumped elements values within$\pm$ 5%. This analysis also revealed 2 crucial elements of the matrix, the values of which need to be known accurately to retain its performance (these may need to be implemented as variable capacitors and inductors).

References: [1] Schneider R (2013). Proc. ISMRM 4252. [2] Kozlov M (2013). Proc. EuMA: 1223 – 1226. [3] Jevtic J (2001). Proc. ISMRM, **17**. [4] Mahmood Z (2013). Proc. ISMRM 2722. [5] Lee R (2002). MRM **48**(1): 203-213

Acknowledgements: NIH support: R01EB0006847, R01EB007942, Siemens-MIT CKI Alliance.

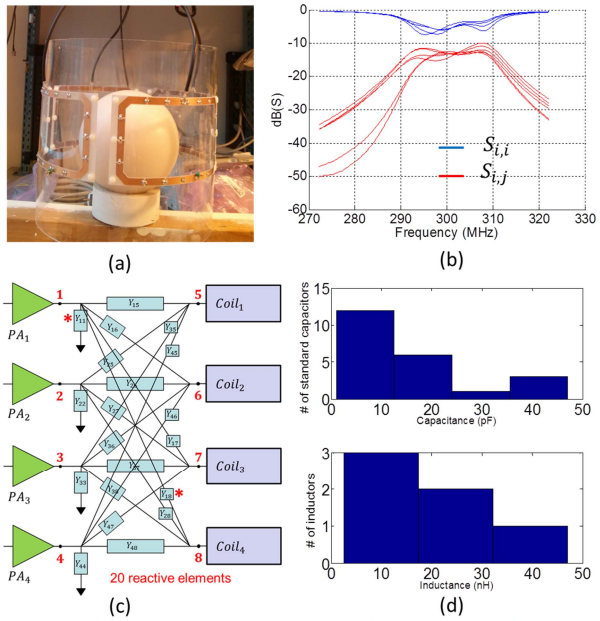

Figure 1: (a) Picture of the coupled 4-channel 7T parallel transmit head array to be decoupled. (b) S-parameters of the array shown in Fig 1(a), $S_{i,i}$ indicates the reflection at port i, while $S_{i,j}$ indicates the coupling between ports i and j. (c) Schematic of the decoupling matrix. The elements $Y_{i,j}$ indicate a reactive element connected between the nodes i and j. (d) Histograms of the calculated standard capacitors and inductors for the decoupling matrix

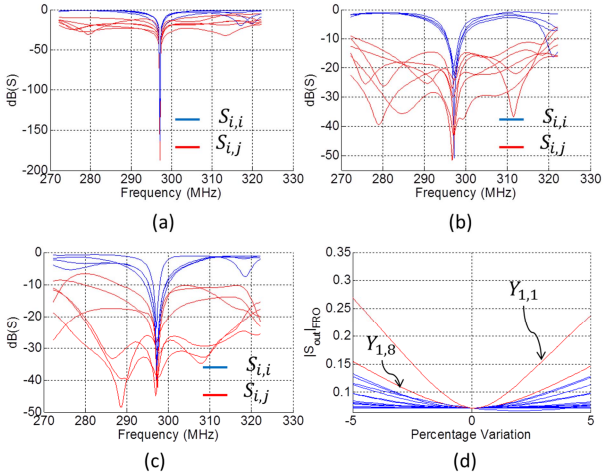

Figure 2: S-parameters of the array with the decoupling matrix (S_{out}) without (a) and with (b) a robustness criterion. (c) S-parameters of the robust matrix populated with capacitors and indictors having only standard values. (d) Variation of the sum of all S-parameters (Frobeneous norm of the output S-matrix) with respect to -5% to +5% variations of the lumped elements (1 curve per lumped element). The red curves indicate lumped elements that are the most critical for good performance of the decoupling matrix. These elements are marked by red asterisks in Fig. 1(c).